Progress In Electromagnetics Research M, Vol. 23, 13–28, 2012

A NEW ALGORITHM FOR ELIMINATING THE FREQUENCY DIFFERENCE IN PHASE NOISE MEASUREMENT OF THE MICROWAVE SIGNAL

X.-L. Chen*, X.-F. Zhang, and J.-L. Wang

School of Mechano-Electronic Engineering, Xidian University, Xi'an 710071, China

Abstract—The frequency difference between signal-under-test and reference signal in phase demodulation will affect the result of the actual phase noise measurement. In order to eliminate the effect, an algorithm for both eliminating the frequency difference and extracting the phase noise of the signal-under-test is presented. Simulation and experiment results show that this algorithm is effective. By using the algorithm in our experiment, the noise floor of the measurement system is improved by 10.1 dB and 9.3 dB, respectively, and the measurement precision is improved from 90.03% to 96.31%. In addition, the use of this algorithm can lower the requirement on the frequency precision of reference source and reduce the cost of measurement system.

1. INTRODUCTION

Phase noise, an important parameter of the oscillator, affects the quality and performance of radio frequency (RF) and microwave system. Its characterization and measurement are, therefore, of great significance in application. The concept and characterization of phase noise have been introduced in detail [1]. Demir and Roychowdhury [2] analyzed the effect of orthogonally decomposed perturbations on phase noise, studied a unifying theory and numerical methods for practical characterization of phase noise in the oscillator, and used several different kinds of perturbations for simulation. Phase noise models have been analyzed in some published papers. The phase noise of the RF oscillator is considered the integration of the frequency noise

Received 22 September 2011, Accepted 27 December 2011, Scheduled 6 January 2012
* Corresponding author: Xiaolong Chen (xlchen@mail.xidian.edu.cn).

which consists of white noise and flicker noise [3]. The phase noise of monolithic voltage-controlled oscillators is formulated with the aid of a linearized model, and a new definition of Q is introduced and simulated in [4]. The correlation theory methods have been used to obtain a model for the near-carrier oscillator based on the measurement-driven representation of phase noise, which is a sum of power-law processes [5]. The general correlation spectrum of an oscillator with white and $f^{-\alpha}$ noise sources is derived from the Langevin equations describing deterministic and stochastic behaviors of an oscillator by perturbation methods. The treatment of $f^{-\alpha}$ noise and influence of finite measuring time on the noise spectra are included in a time domain calculation [6]. Ward and Duwel [7] presented a systematic construction of an analytical model encompassing the nonlinearity of oscillator phase noise, which provides a transparent connection between oscillator phase noise and fundamental device physics and noise processes. Rizzoli et al. [8] analyzed the numerical optimization of microwave oscillators including specifications on steady-state stability and near carrier phase noise, using the harmonic-balance technique. These works provide a valuable theoretical foundation for research on phase noise measurement. Various phase noise measurement methods have been proposed. There are three main methods: spectrum analyzer method, frequency demodulation method, and phase demodulation method. The spectrum analyzer method, which only requires a spectrum analyzer and a computer, does not need an extra reference source and adopts a modern spectrum analyzer to acquire IQ data to calculate phase noise [9, 10]. This method is easy to set up since no design or construction is required, and the spectrum analyzer is readily available. However, it is severely limited due to the fact that the phase noise and amplitude noise of the local oscillator are indistinguishable in the spectrum analyzer and that the close-in phase noise is immeasurable. The frequency demodulation method is the only method that requires no reference source, and it is suitable for measuring large phase deviations at low rates. The dual photonic-delay line cross correlation method of frequency demodulation for phase noise measurement, which combines delay-line discriminator and cross-correlation by using low-loss kilometer-long photonic delay, is described in [11, 12]. Rubiola and Budot analyzed phase noise measurement methods in which correlation and averaging are adopted to reject both the background noise of the instrument and the effect of AM noise on correlation phase noise measurement [13]. Normally the delay line frequency discriminator method can be used to measure the frequency drifting signal [14–16]. Owing to the fact that numerous delay lines with different line lengths are needed and that quadrature

adjustment is required, this method is complicated to operate. In phase demodulation method, an additional period is locked to the oscillator under test, and the outputs of the two oscillators are applied to a phase detector, which is usually a double balanced mixer. A phase detector output proportional to the oscillator phase noise is applied to a low noise amplifier. Ultimately, the amplified signal is applied to a spectrometer, which is a spectrum analyzer or a digital FFT analyzer. The phase noise measurement in the frequency domain and phase demodulation method are introduced [17].

In using the phase demodulation method for phase noise measurement, the reference signal must be exactly equal in frequency to the signal-under-test. The PLL is used to ensure that the reference signal is equal in frequency to the signal-under-test. However, in actual measurement, the PLL does not always ensure the equality. The frequency difference between the signal-under-test and the reference signal will affect the result of phase noise measurement. In order to eliminate the effect of the frequency difference, we have developed an algorithm for both eliminating the frequency difference and extracting the phase signal.

This paper is organized as follows. Section 2 introduces the principle of the frequency difference elimination algorithm. Section 3 describes the simulated and experimental results of this algorithm. The conclusion of this paper is presented in Section 4.

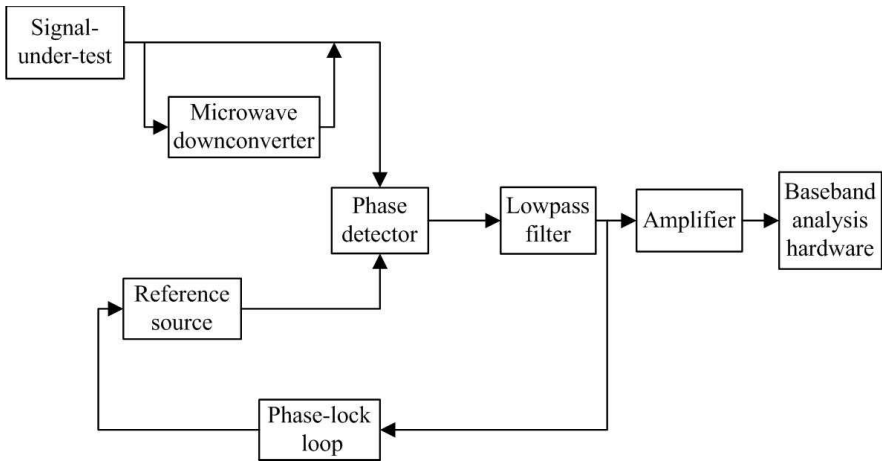

Figure 1. The diagram of the phase demodulation method.

2. THE FREQUENCY DIFFERENCE ELIMINATION ALGORITHM

The diagram of phase demodulation method is shown in Figure 1. In the diagram, the reference signal is set at the same frequency and quadrature as the signal-under-test. The reference signal should have less noise than the signal-under-test. Otherwise, the sum of the noise of the two sources would be measured. It can be seen from Figure 1 that the PLL provides necessary feedback for the reference source in order to maintain the same frequency and quadrature as that of the signal-under-test. However, as mentioned above, the PLL could not always ensure that the signal-under-test is exactly equal in frequency to the reference signal in actual measurement. Our algorithm for eliminating the effect of the frequency difference on phase noise measurement is made up of two parts: extracting phase noise from the signal containing frequency difference and estimating the signal parameter.

2.1. Extracting Phase Noise from the Signal Containing Frequency Difference

Assume the signal-under-test and the reference signal as follow:

$$V_i(t) = A_i \sin[\omega_i t + \theta_i + \phi_i(t)] \tag{1}$$

$$V_r(t) = A_r \sin\left[\omega_r t + \theta_r + \frac{\pi}{2} + \phi_r(t)\right] = A_r \cos[\omega_r t + \theta_r + \phi_r(t)] \tag{2}$$

where $V_i(t)$ is the signal-under-test, θ_i the initial phase of the signal-under-test, $\phi_i(t)$ the phase noise of the signal-under-test, $V_r(t)$ the reference signal, $\theta_r + \frac{\pi}{2}$ the initial phase of the reference signal, and $\phi_r(t)$ the phase noise of the reference signal.

Then the output of the phase detector is $V_d(t)$:

$$\begin{aligned} V_d(t) &= V_i(t) \cdot V_r(t) \\ &= A_i \cdot A_r \sin[\omega_i t + \theta_i + \phi_i(t)] \cos[\omega_r t + \theta_r + \phi_r(t)] \\ &= \frac{1}{2} A_i \cdot A_r \{\sin[(\omega_i + \omega_r)t + \theta_i + \theta_r + \phi_i(t) + \phi_r(t)] \\ &\quad + \sin[(\omega_i - \omega_r)t + \theta_i - \theta_r + \phi_i(t) - \phi_r(t)]\} \end{aligned} \tag{3}$$

Through the low-pass filter, the output of the low-pass filter is $y(t)$:

$$\begin{aligned} y(t) &= A \sin[(\omega_i - \omega_r)t + \theta_i - \theta_r + \phi_i(t) - \phi_r(t)] \\ &= A \sin[\Delta\omega t + \theta_0 + \phi(t)] \end{aligned} \tag{4}$$

where A is the amplitude of the signal $y(t)$, $\Delta\omega$ the frequency difference between the signal-under-test and the reference signal, θ_0 the original phase difference between the signal-under-test and the reference signal,

and $\phi(t) = \phi_i(t) - \phi_r(t)$ the phase noise of the signal-under-test relative to the reference signal.

There may be a direct current component in actual measurement, so Equation (4) can be rewritten as:

$$y(t) = A\sin(\Delta\omega t + \theta_0 + \phi(t)) + C \tag{5}$$

where C is the direct current component.

According to the law of sine, Equation (5) could be rewritten as:

$$y(t) = A\sin(\Delta\omega t + \theta_0)\cos(\phi(t)) + A\cos(\Delta\omega t + \theta_0)\sin(\phi(t)) + C \tag{6}$$

In ideal conditions, $\Delta\omega = 0$, $\theta_0 = 0$, $\phi(t) \ll 1$, $\cos(\phi(t)) \approx 1$, and $\sin(\phi(t)) \approx \phi(t)$, and then the signal which contains phase noise can be expressed by Equation (7):

$$y(t) = A\sin(\phi(t)) + C \approx A\phi(t) + C \tag{7}$$

According to Equation (7), the power spectral density (PSD) of the phase noise signal $\phi(t)$ could be computed by the PSD of $y(t)$.

In actual measurement, however, $\Delta\omega \neq 0$, $\theta_0 \neq 0$, $\phi(t) \ll 1$, $\cos(\phi(t)) \approx 1$, and $\sin(\phi(t)) \approx \phi(t)$, and then Equation (6) can be rewritten as:

$$y(t) \approx A\sin(\Delta\omega t + \theta_0) + A\cos(\Delta\omega t + \theta_0)\phi(t) + C \tag{8}$$

Therefore, the PSD of the phase noise signal cannot be replaced by the PSD of $y(t)$. In some published papers, the PSD of $y(t)$, instead of the phase noise of the measured signal, is used, which is not strict, especially when the frequency difference $\Delta\omega$ is large. In order to extract the phase noise signal $\phi(t)$ from the low-pass filter output $y(t)$, the effect of the frequency difference on phase noise measurement must be eliminated. Our algorithm is used to eliminate the frequency difference in Equation (8).

From Equation (8), the $\phi(t)$ can be found in Equation (9).

$$\phi(t) = \frac{y(t) - A\sin(\Delta\omega t + \theta_0) - C}{A\cos(\Delta\omega t + \theta_0)} \tag{9}$$

If parameters A, $\Delta\omega$, θ_0 and C in Equation (9) can be estimated by the measured data, the phase noise could be computed by Equation (10).

$$\phi(t) = \frac{y(t) - \hat{A}\sin(\hat{\Delta\omega} t + \hat{\theta_0}) - \hat{C}}{\hat{A}\cos(\hat{\Delta\omega} t + \hat{\theta_0})} \tag{10}$$

where $\hat{A}$, $\hat{\Delta\omega}$, $\hat{\theta_0}$ and $\hat{C}$ are the estimated values of A, $\Delta\omega$, θ_0 and C, respectively.

2.2. Estimating the Signal Parameter

Some methods are used to estimate the parameter in some papers. The frequency of the signal is estimated by measuring microwave power difference [18]. The four-parameter estimation of the sine model is used to estimate both the frequency of sine by the FFT of the sampled signal and the other three parameters according to the frequency in the sine model [19]. In this paper, the method is improved to estimate the parameters of the non-sine signal, such as A, $\Delta\omega$, θ_0 and C in Equation (8). Then by Equation (10), the phase noise signal $\phi(t)$ can be extracted from $y(t)$. In this paper, the estimated signal is given as:

$$\begin{aligned} y(k) &= A\sin(\Delta\omega t_k + \theta_0) + C \\ &= A\cos\theta_0 \sin(\Delta\omega t_k) + A\sin\theta_0 \cos(\Delta\omega t_k) + C \\ &= P\sin(\Delta\omega t_k) + Q\cos(\Delta\omega t_k) + C \end{aligned} \tag{11}$$

where $P = A\cos\theta_0$, $Q = A\sin\theta_0$, and k is the serial number of sampling data. The main steps of signal parameter estimation are summarized as follow:

(1) Estimating the approximate range of the frequency of the signal, expressed as $[\omega_{0l}, \omega_{0h}]$, and the initial value of frequency, expressed as $\Delta\hat{\omega}_0$, i being the times of the iteration and the first iterating time $i = 0$. The initial deviation error of the frequency estimation is expressed as $\delta\omega_0$, and then $\delta\omega_0 = \omega_{0h} - \omega_{0l}$.

(2) Letting $i = i + 1$, $\omega_{il} = \Delta\hat{\omega}_{i-1} - \delta\omega_0/M^{i-1}$, and $\omega_{ih} = \Delta\hat{\omega}_{i-1} + \delta\omega_0/M^{i-1}$, where the number M describes the search step length of frequency. The larger is the M, the shorter is the search step length. In this paper, the value of number M is 5 in the experiment.

(3) $2M + 1$ frequency values selected from the frequency range $[\omega_{il}, \omega_{ih}]$, expressed as $\Delta\omega_{ij}$, $j = 0, 1, \ldots, 2M$, and calculating the parameters A_{ij}, θ_{ij}, C_{ij} and the square error E_{ij} by Equations (12), (13), (14), (15) and (16).
In the least square solution, the A_{ij}, θ_{ij} and C_{ij} can be estimated by the following equations. Let

$$D_{ij} = \begin{bmatrix} \cos(\Delta\omega_{ij}t_0) & \sin(\Delta\omega_{ij}t_0) & 1 \\ \cos(\Delta\omega_{ij}t_1) & \sin(\Delta\omega_{ij}t_1) & 1 \\ \vdots & \vdots & \vdots \\ \cos(\Delta\omega_{ij}t_{N-1}) & \sin(\Delta\omega_{ij}t_{N-1}) & 1 \end{bmatrix} \tag{12}$$

$$Y = \begin{bmatrix} y(0) \\ y(1) \\ \cdots \\ y(N-1) \end{bmatrix} \tag{13}$$

Then

$$\begin{bmatrix} P_{ij} \\ Q_{ij} \\ C_{ij} \end{bmatrix} = \left(D_{ij}^T D_{ij}\right)^{-1} \left(D_{ij}^T Y\right) \tag{14}$$

where D_{ij}^T is the transposition of D_{ij}. Then A_{ij} and θ_{ij} can be written as these equations:

$$A_{ij} = \sqrt{P_{ij}^2 + Q_{ij}^2}, \quad \theta_{ij} = \arcsin\left(\frac{Q_{ij}}{A_{ij}}\right) \tag{15}$$

The square mean error is calculated in the following equation:

$$\begin{aligned} E_{ij} &= \sum_k \left(y(t_k) - A_{ij}\sin(\Delta\omega_{ij}t_k + \theta_{ij}) - C_{ij}\right)^2 \\ &= \sum_k (y(t_k) - P_{ij}\sin(\Delta\omega_{ij}t_k) - Q_{ij}\cos(\Delta\omega_{ij}t_k) - C_{ij})^2 \end{aligned} \tag{16}$$

where k is the serial number of the sampling data.

(4) Comparing the square errors of the $2M + 1$ frequency values in Step (3), and then finding the frequency value with the minimum square error, expressed as $\Delta\hat{\omega}_i$, and its three parameters, expressed as $\hat{A}_i$, $\hat{\theta}_i$ and $\hat{C}_i$. This is the estimation of the four parameters of the signal for the ith iteration, and the maximum deviation error of the frequency estimation is given as $\delta\omega_i = \delta\omega_0/M^i$.

(5) Repeating Steps (2)–(4) until the frequency which satisfies the allowable error is found and thus $\Delta\hat{\omega}$, $\hat{A}$, $\hat{\theta}_0$ and $\hat{C}$ are found.

(6) By substituting $\Delta\hat{\omega}$, $\hat{A}$, $\hat{\theta}_0$ and $\hat{C}$ into Equation (10), the estimation of the phase noise signal can be achieved.

In actual measurement, an allowable error of the phase noise is given. In Step (5), the allowable error of the frequency is determined by that of the phase noise. The following equations are used to determine the allowable error of the frequency.

From Equation (10) and the error transform equation, the error of a frequency can be expressed by:

$$\begin{aligned} \delta_\phi \;=\; & \frac{\hat{C} - y(t)}{\hat{A}^2\cos(\hat{\Delta\omega}t + \hat{\theta}_0)}\delta_A + \frac{t(y(t) - \hat{C})\sin(\hat{\Delta\omega}t + \hat{\theta}_0) - \hat{A}t}{\hat{A}\cos^2(\hat{\Delta\omega}t + \hat{\theta}_0)}\delta_\omega \\ & + \frac{(y(t) - \hat{C})\sin(\hat{\Delta\omega}t + \hat{\theta}_0) - \hat{A}}{\hat{A}\cos^2(\hat{\Delta\omega}t + \hat{\theta}_0)}\delta_{\theta_0} + \frac{-1}{\hat{A}\cos(\hat{\Delta\omega}t + \hat{\theta}_0)}\delta_C \end{aligned} \tag{17}$$

$$\begin{cases} \delta_A \approx \hat{A}(t/2)\delta_\omega \\ \delta_{\theta_0} \approx \hat{\theta}_0(t/2)\delta_\omega \end{cases} \tag{18}$$

where δ_ϕ is the error of the phase noise, δ_A the error of amplitude of the signal, δ_ω the error of the frequency, δ_{θ_0} the error of the initial phase, and δ_C the error of the direct current component.

Substituting Equation (18) into Equation (17), the allowable error of the frequency can be found by that of the phase noise.

3. SIMULATION AND EXPERIMENTS

In order to validate the performance of our algorithm, we present the simulated and experimental results as follows. A sinusoidal signal model which is modulated by a given signal as phase noise is used for simulation, and then the actual measurement data with phase noise are used for experimentation.

The simulation signal is given as:

$$y(t) = A\sin(\Delta\omega t + \theta_0 + \phi(t)) + C \tag{19}$$

where $A = 2$, $\Delta\omega = 40\pi\,\text{rad/s}$, $\theta_0 = 0.8727\,\text{rad/s}$ and $C = 2$.

The simulated signals are generated by modulating four types of phase noise $\phi(t)$ to the sine signal $y(t)$ as Equation (19). There are four signals used as phase noise $\phi(t)$ in the simulation: randn(t) generates a random signal whose sequence is normally distributed; $\sin(2\pi t)$ generates a sequence sine wave; rand(t) generates pseudorandom numbers whose sequence is uniformly distributed; chirp(t) generates a sequence swept-frequency cosine. They are the function of the MatLab. The sampling frequency is 1 kHz. The simulation result is shown in Figure 2.

Figure 2 shows the simulation result of the four types of modulated phase noise signal. In each sub-figure of Figure 2, the up curve is the simulation signal, middle curve the given phase noise signal in simulation, and down curve the extracted phase noise signal by our algorithm. The mean square error of the given phase noise signal and extracted phase noise signal by our algorithm is shown in Table 1. The simulation result shows that the frequency difference is eliminated and that the phase noise signal is extracted effectively by the algorithm.

An experiment which uses the real measured data with phase noise is implemented in this paper. The operation frequency in the experiment is 600 MHz. In order to compare the measured result of

Table 1. The mean square error of the given phase noise signal and extracted phase noise signal.

The simulation in Figure 2	(a)	(b)	(c)	(d)
The mean square error $[10^{-6}]$	1.19580	0.30721	0.40462	0.38037

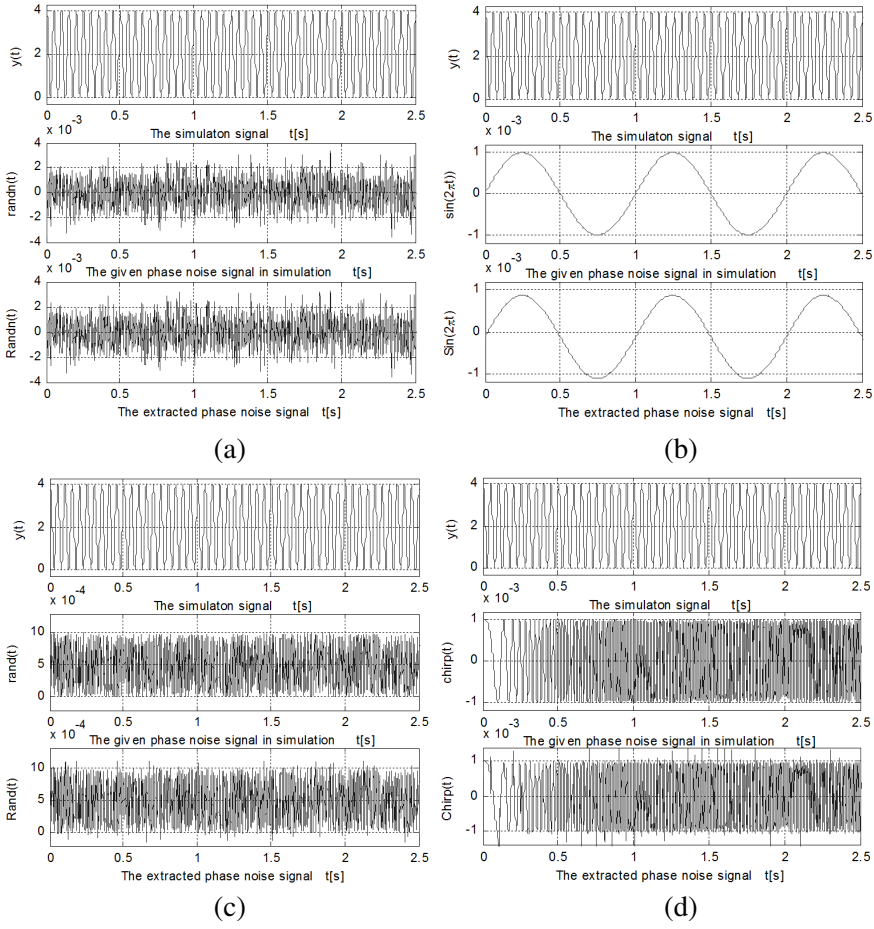

Figure 2. Simulation result.

the close-to-carrier wave and far-from-carrier wave, the two sampling frequencies, 10 kHz and 1 MHz, are used in the experiment. The experiment is performed by flow "a" in Figure 3. The signal-under-test and the reference signal are generated by the signal source AV1485 and AV1463, respectively. The phase detector is made up of two semiconductor diodes HMS2823. Figure 4 shows the circuit layout of phase demodulation, low-pass-filter, and low noise amplifier. Then the amplified signal is sampled by the Tektronix DPO7254 and imputed into a computer. The sampling data are first processed by our algorithm to eliminate frequency difference and extract phase noise.

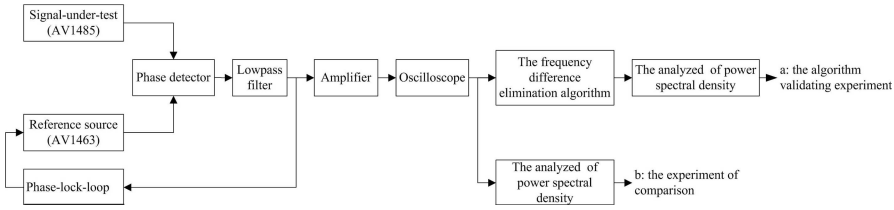

Figure 3. The flows of the experiment using our algorithm and the experiment by the conventional phase demodulation method not using our algorithm.

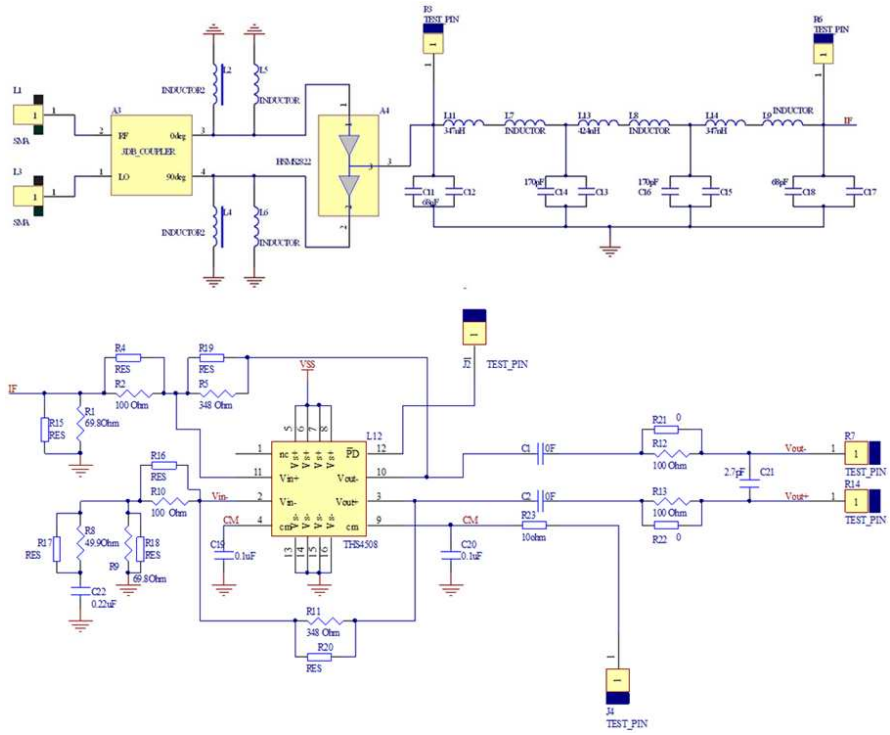

Figure 4. Circuit layout for our experiment.

After that, they are used to estimate the power spectral density. As an experiment of comparison, as flow "b" in Figure 3, the same sampling data are used directly to estimate the power spectral density by the conventional phase demodulation without processing them by our algorithm.

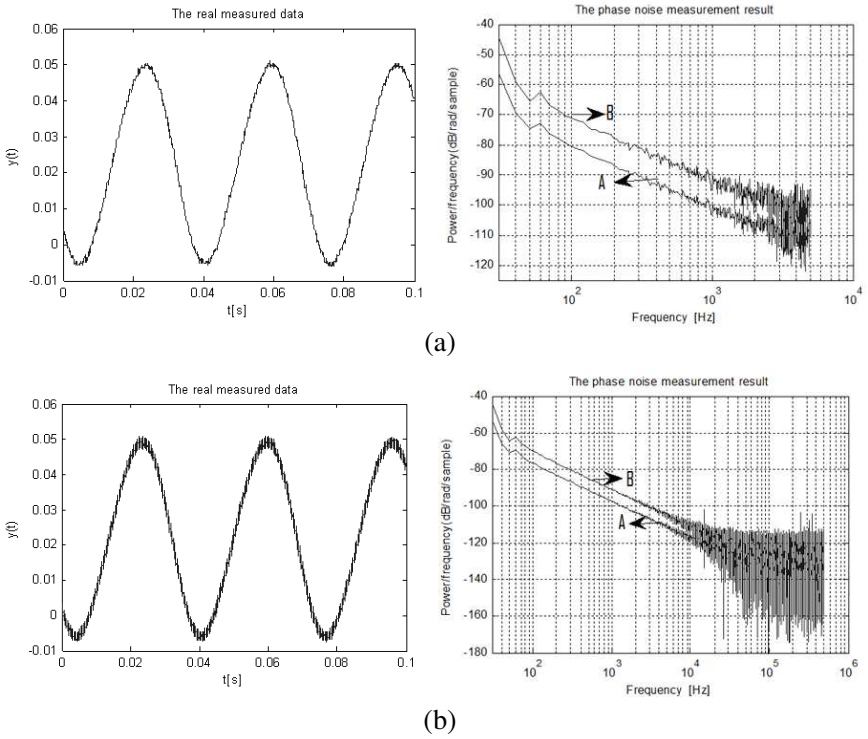

Figure 5. Real measured data and phase noise measurement result. (a) The sampling frequency is 10 kHz. (b) The sampling frequency is 1 MHz.

The real measured data and phase noise measurement result are shown in Figure 5. In each sub-figure of Figure 5, the real measured signal is indicated in the left figure, and the phase noise measurement result of the real measured signal is shown in the right figure. In the right sub-figures of Figure 5, Curve A stands for the phase noise measurement result by the "a" experiment flow, which is treated by our algorithm, and Curve B stands for the phase noise measurement result by the "b" experiment flow, which is not treated by the algorithm. A comparison of the phase noise measurement results at some frequency points is given in Tables 2 and 3. The phase noise measurement result by spectral analyzer AV4036 is given in these tables as a reference value. Spectral analyzer AV4036, which is a synthetical measurement instrument, has a special module to be used to measure the phase noise of the signal. The signal-under-test is generated by the signal source AV1485, which has a low amplitude noise far less than that of the

Table 2. A comparison of the phase noise measurement results at some frequency points with the sampling frequency being 10 kHz.

Frequency [Hz]	100	500	1000	2500	5000	MSE[a]	Noise floor
The measurement result by spectral analyzer AV4036 [dB]	−90.12	−98.30	−100.67	−105.52	−108.63	−−	−123.6
The measurement result not treated by the algorithm [dB]	−71.06	−87.49	−94.87	−95.64	−99.05	−−	−98.3
The measurement error with the result by AV4036 as a reference value [dB]	19.06	10.81	5.8	9.88	9.58	10.25	−−
The measurement result treated by the algorithm [dB]	−80.43	−96.07	−102.9	−111.70	−109.7	−−	−108.4
The measurement error with the result by AV4036 as a reference value [dB]	9.69	2.23	−2.23	−6.18	−1.07	3.17	−−

Note a: The measurement errors at different frequency points are averaged for a visualized comparison between the measurement result not treated by the algorithm and that treated by the algorithm.

phase noise. The effect of the amplitude noise of the signal-under-test on the experiment result is negligible. Therefore, the measured result by AV4036 is used as a reference value which indicates the precision of the experiment result.

In Tables 2 and 3, the experiment results at different frequency points are used to calculate the measurement error and show the performance of our algorithm. According to Table 2, with the sampling frequency being 10 kHz, the noise floor of the measurement system is −98.3 dB before the measurement data are treated by the algorithm.

Table 3. A comparison of the phase noise measurement results at some frequency points with the sampling frequency being 1 MHz.

Frequency [Hz]	500	1000	2500	5000	10000	MSE	Noise floor
The measurement result by spectral analyzer AV4036 [dB]	−98.30	−100.67	−105.52	−108.63	−116.57	−−	−123.6
The measurement result not treated by the algorithm [dB]	−84.67	−90.79	−98.49	−104.40	−105.69	−−	−113.2
The measurement error with the result by AV4036 as a reference value [dB]	13.63	9.88	7.03	4.23	10.88	8.47	−−
The measurement result treated by the algorithm [dB]	−91.13	−97.28	−105.10	−110.90	−118.50	−−	−122.5
The measurement error with the result by AV4036 as a reference value [dB]	7.17	3.39	0.42	−2.27	−1.93	2.14	−−

By using our algorithm, the noise floor is decreased to −108.4 dB, which is an improvement of 10.1 dB. With the measurement result by AV4036 as a reference value, the Mean Squared Error (MSE) of measurement not treated by the algorithm is 10.25, and that treated by the algorithm is 3.17. Similarly, according to Table 3, with the sampling frequency being 1 MHz, the noise floor of the measurement system is −113.2 dB before the measurement data are treated by the algorithm. By using our algorithm, the noise floor is decreased to −122.5 dB, which is an improvement of 9.3 dB. With the measurement result by AV4036 as a reference value, the MSE of measurement not treated by the algorithm is 8.47, and that treated by the algorithm is 2.14.

Figure 5, Tables 2 and 3 reveal that the phase noise of the real

measured signal can be extracted and measured effectively by our algorithm. According to the experiment scheme above, the circuit layout and the method of estimating power spectral density in the algorithm validating experiment are the same as that in the experiment of comparison. The exclusive difference between the two experiments is that the experiment of comparison does not use our algorithm. Therefore, the improved measurement performance, besides noise floor and precision, of experiment "a" compared to experiment "b" is caused by our algorithm. Corresponding to sampling frequency, the analyzed band range of the experiment data shown in Table 2 is 100 Hz $\sim$ 5 kHz, while the experiment data shown in Table 3 are 500 Hz $\sim$ 500 kHz. The experiment result shows that the algorithm has equal measuring capability for close-to-carrier and far-from-carrier phase noise.

4. CONCLUSION

The phase demodulation method is one of the most commonly used methods in phase noise measurement, in which the reference source is required to be equal in frequency to the signal-under-test. However, in actual measurement the PLL does not always ensure that the reference signal is precisely equal in frequency to the signal-under-test. This paper presents a new algorithm for eliminating the effect of the frequency difference between the signal-under-test and the reference signal in phase noise measurement. The simulated and experimental results show that the frequency difference can be removed with the phase noise extracted effectively. In our experiment, the phase noise floor is improved by 10.1 dB and 9.3 dB, respectively by using our algorithm. With the measurement result by AV4036 as a reference value, the measurement precision is improved from 90.03% to 96.31%. The algorithm has equal measuring capability for close-to-carrier and far-from-carrier phase noise. Even if the frequency of the reference source is not steady enough, the measurement data can be dealt with by using our algorithm to improve the phase noise measurement result. Therefore, the requirement on frequency stability of the reference source can be lowered, and the cost of the measurement system can be reduced.

ACKNOWLEDGMENT

The authors would like to thank the editors and reviewers for their valuable and insightful comments. This research was supported by the Fundamental Research Funds for the Central Universities under Grant No. K50510040011.

REFERENCES

1. Barnes, J. A., A. R. Chi, L. S. Cutler, et al., "Characterization of frequency stability," *IEEE Transactions on Instrumentation and Measurement*, Vol. 20, No. 2, 105–120, 1971.
2. Demir, A. and J. Roychowdhury, "On the validity of orthogonally decomposed perturbations in phase noise analysis," *Technical Memorandum*, 1–13, Bell Laboratories, Murray Hill, 1997.
3. Yousefi, S., T. Eriksson, and D. Kuylenstierna, "A novel model for simulation of RF oscillator phase noise," *2010 IEEE Radio and Wireless Symposium*, 428–431, 2010.
4. Razavi, B., "Analysis, modeling, and simulation of phase noise in monolithic voltage-controlled oscillators," *Proceedings of the IEEE Custom Integrated Circuits Conference*, 323–326, 1995.
5. Chorti, A. and M. Brookes, "A spectral model for RF oscillators with power-law phase noise," *IEEE Transactions on Circuits and Systems I: Regular Papers*, Vol. 53, No. 9, 1989–1999, 2006.
6. Kaertner, F. X., "Analysis of white and $f^{-\alpha}$ noise in oscillators," *International Journal of Circuit Theory and Application*, 485–519, 1990.
7. Ward, P. and A. Duwel, "Oscillator phase noise: Systematic construction of an analytical model encompassing nonlinearity," *IEEE Transaction on Ultrasonics, Ferroelectrics, and Frequency Control*, Vol. 58, No. 1, 195–205, 2011.
8. Rizzoli, V., A. Costanzo, F. Mastri, et al., "Harmonic-balance optimization of microwave oscillators for electrical performance, steady-state stability, and near-carrier phase noise," *IEEE MTT-S International Microwave Symposium Digest*, 1401–1404, 1994.
9. Chen, J., F. Jonsson, and L. R. Zheng, "A fast and accurate phase noise measurement of free running oscillators using a single spectrum analyzer," *2010 IEEE Norchip Conferences*, 1–4, 2010.
10. Angrisani, L., A. Baccigalupi, and M. D'Arco, "A new method for phase noise measurement," *Proceedings of the 19th IEEE Instrumentation and Measurement Technology Conference*, Vol. 1, 663–668, Anchorage, AK, USA, 2002.
11. Salik, E., N. Yu, and L. Maleki, "Dual photonic-delay line cross correlation method for phase noise measurement," *Proceedings of the 2004 IEEE International Frequency Control Symposium and Exposition*, 303–306, 2004.
12. Rubiola, E., E. Sailk, S. H. Huang, et al., "Photonic delay technique for phase noise measurement of microwave oscillators," *Optics InfoBase JOSA B*, Vol. 22, No. 5, 987–997, 2005.

13. Rubiola, E. and R. Boudot, "The effect of AM noise on correlation phase-noise measurements," *IEEE Transactions on Ultrasonics, Ferroelectrics, and Frequency Control*, Vol. 54, No. 5, 926–932, 2007.
14. Stein, S. R., "Frequency and time: Their measurement and characterization," *Precision Frequency Control*, Vol. 2, 191–232, 1985.
15. Walls, F. L. and E. S. Ferre-Pikal, "Measurement of frequency, phase noise and amplitude noise," *The Wiley Encyclopedia of Electrical and Electronic Engineering*, Vol. 12, 459–473, 1999.
16. Gheidi, H. and A. Banai, "A new phase shifter-lee delay line method for phase noise measurement of microwave oscillators," *Proceeding of the 38th European Microwave Conference*, 325–328, Amsterdam, The Netherlands, 2008.
17. Lance, A., D. S. Wendell, and F. Labaar, "Phase noise and AM noise measurements in the frequency domain," *Infrared and Millimeter Waves*, Vol. 11, 239–289, 1984.
18. Ni, J., X. M. Zhang, S. L. Zheng, X. F. Jin, H. Chi, and X. M. Zhang, "Microwave frequency measurement based on phase modulation to intensity modulation conversion using fiber bragg grating," *Journal of Electromagnetic Waves and Applications*, Vol. 25, Nos. 5–6, 755–764, 2011.
19. Händel, P., "Properties of the IEEE-STD-1057 four-parameter sine wave fit algorithm," *IEEE Transaction on Instrumentation and Measurement*, Vol. 49, No. 6, 1189–1193, 2000.